EFFECT OF SPIN AND YAW ON BOUNDARY LAYER TRANSITION ALONG A BODY OF REVOLUTION

Thesis by

Alvin L. Fehrman

Captain, U. S. Air Force

In Partial Fulfillment of the Requirements

For the Degree of

Aeronautical Engineer

California Institute of Technology

Pasadena, California

1955

ACKNOWLEDGEMENTS

The author wishes to express his appreciation to the members of the staff of the Guggenheim Aeronautical Laboratory, California Institute of Technology for their able assistance and suggestions which made possible the investigation herein reported.

In particular, he wishes to thank Dr. C. B. Millikan, Director of the Laboratory and Dr. A. Roshko under whose supervision the project was undertaken. He also wishes to thank Dr. H. J. Stewart and Dr. V. A. Vanoni for their many suggestions, and Mr. H. C. Thorman who was responsible for the design and maintenance of much of the apparatus used.

SUMMARY

This report covers an experimental investigation of boundary layer transition on a body of revolution at low subsonic speeds, with emphasis placed on the effects of spin and yaw on transition.

The methods tried for detecting boundary layer transition for this particular investigation are reviewed and the technique finally adopted, the use of a hot wire anemometer, is described in detail.

It was found that at angles of yaw, the transition from laminar to turbulent flow in the boundary layer occurs at a higher Reynolds number over most of the body than at zero yaw, and that spin has a negligible effect on the transition Reynolds number. It was observed however that the effect of spin varies from the front to the rear of the body, although it was not ascertained whether this effect was a result of the influence of the nose section, the tripping device which was used to obtain transition, or a combination of both.

TABLE OF CONTENTS

SYMBOLS

d	=	model diameter
rps	=	revolutions per second
Re_d	=	$\frac{Ud}{\nu}$
Re_x	=	$\frac{UX}{\nu}$
L	=	model length
U	=	free stream velocity
X	=	axial distance from model nose
α	=	angle of yaw of model
ν	=	kinematic viscosity - free stream
ω	=	spin rate of model in r.p.s., defined positive when the crossflow velocity component relative to the model lower surface is increased.

I. INTRODUCTION

The present investigation was initiated with the purpose of studying boundary layer transition on a body of revolution at low subsonic speeds by use of experimental methods, and in particular to determine the effects of spin and yaw on such transition.

At the time this project was initiated, an investigation was being conducted at the California Institute of Technology for the purpose of studying the Magnus force and moment on a yawed rotating body of revolution. It was felt that a knowledge of the effects of spin and yaw on boundary layer transition might be of value to such an investigation. In addition the skin friction coefficient and, as a result, the drag of a body having a turbulent boundary layer is higher than that having a laminar boundary layer. For this reason it is advantageous to be able to predict the type of boundary layer to be expected on a missile or aircraft, especially during the design stages.

The mechanism of transition is not completely understood, and consequently most of the material currently available on this subject has been obtained experimentally. A survey of the literature shows that very little information is available for bodies of revolution. It is hoped that the results of this investigation may add a small contribution to the current subject matter on boundary layer transition along a body of revolution, and in particular be of value for the above mentioned purposes.

II. DESCRIPTION OF APPARATUS

1. Test Facilities:

The results reported herein were obtained in the Merrill Wind Tunnel which is designed for speeds up to 250 ft. per second. It is a closed return tunnel having a 32 by 45 inch atmospheric test section. Three screens were used in order to obtain a reduced turbulence level. For a more detailed description of the characteristics of the tunnel the reader is referred to reference 1.

2. Model:

The model and mounting used were originally designed by Dr. George Solomon. The original design with modifications were used to conduct the tests for this study.

The model shown in Figure 1 consists of two sections, the body section and the nose section. The body section is basically a cylindrical can made of lucite. This can is supported by an axial, hollow strut. A shaft within the strut rotates the can about its axis.

The can is constructed so that a variety of nose section shapes may be attached to it. An elliptic nose section constructed of wood was used for the tests herein reported. The overall length of the model is 24 inches and its diameter is 2.4 inches. The nose section is 3 diameters or 7.2 inches in length.

3. Provision for Rotation:

The model drive shaft is connected through a 5 to 1 speed reducer to a series wound direct current motor rated 1/13 horsepower at 8500 rpm. Power was supplied to the motor through a powerstat and from a 12 volt rectifier, the powerstat being used for rotational

control. An electronic counter was used to determine the model rotational speed. A ten-toothed disc attached to the drive shaft induced a voltage in a magnetic pickup and thereby supplied a signal to the electronic counter.

4. Provisions for Yaw:

The model shaft is attached by means of a cantilever to a vertical supporting system so that it may be yawed up to a maximum of 20 degrees to either side in a horizontal plane. The vertical supporting members are attached to a steel base plate.

5. Model Installation:

The model assembly was installed in the tunnel by mounting the base plate on a tubular steel frame which rested on the floor of the tunnel housing. The steel frame was somewhat flexible so as to damp out vibrations which might otherwise be transmitted from the floor to the model, however some vibrations did occur at high velocities as a result of this feature.

6. Hot Wire Equipment:

A platinum - $10^{o}/o$ rhodium wire, 0.0002 inches in diameter and 1/8 inch in length was used to determine whether the boundary layer flow was laminar or turbulent. The hot wire probe was mounted on a leadscrew which was attached to the test section floor. A flexible cable attached to the leadscrew was used to traverse the hot wire axially along the model from outside the tunnel.

A standard hot wire circuit giving a range of current up to 150 milliamperes was used. The hot wire signal was fed into both an oscilloscope and a r.m.s. voltmeter through an amplifier. No com-

pensation was required since only a comparison of fluctuations was desired rather than absolute values.

Figure 2 shows the model and hot wire installed in the tunnel and Figure 3 shows the auxiliary equipment used.

III. TEST PROCEDURES

1. Tuft Studies:

As a preliminary method of studying the effects of yaw on the flow pattern around the model, visual observations were made of the patterns formed by cotton tufts attached to the model. These observations were made without spin at several tunnel velocities and angles of yaw up to fifteen degrees. Representative tuft formations obtained in this manner are shown in Figures 4 through 7.

2. Methods Investigated for Detection of Boundary Layer Transition:

Several methods of detecting boundary layer transition were studied in order to determine which method would be most suitable for the particular conditions of this investigation. The methods studied were as follows:

(a) Luminescent Lacquer - Boundary layer transition may be observed visually by the use of a lacquer mixture which has a fluorescent property when dry and irradiated by an ultraviolet light, and which does not possess this property when wet. Since the heat transfer rate in a turbulent boundary layer is higher than that in a laminar boundary layer, turbulence may be detected visually by use of such a lacquer. At the time this method was considered, the model was finished with a lacquer and the primary concern was that the solvent contained in the luminous lacquer mixture might possibly attack this finish. For this reason a piece of wood having the same finish as the model was installed in the tunnel to determine whether a mixture with a reasonable drying time could be obtained for the present study. It was

determined that such a mixture could be obtained which had excellent photographic properties; however, it did attack the lacquer finish. Although this method proved to be an excellent way to study the transition region and to obtain a permanent record in the form of photographs, it was not adaptable to the present study since the procedure requires more time than other methods to obtain the location of the transition region. A complete discussion of this method of studying boundary layer transition is presented in references 2 and 3.

(b) Stethoscope - Boundary layer transition may also be determined by use of a total-head tube attached to a stethoscope. With such a device, a steady noise may be detected when the probe is in a turbulent boundary layer. This method did not prove to be satisfactory for the present study due to the high general noise level in the Merrill Wind Tunnel which is caused by the tunnel motor and fan.

(c) Hot Wire Anemometer - The method adopted for determination of boundary layer transition involved the use of a hot wire anemometer. With a standard hot wire circuit, velocity fluctuations may be observed visually as voltage fluctuations on either an oscilloscope or an r.m.s. voltmeter. A complete review of the basic principles of hot wire anemometry is given in references 4, 5, and 6.

For the present investigation, a 0.0002 inch diameter wire was operated at constant current of 70 milliamperes. Initially a 0.0001 inch diameter wire was used; however, it was found that this size was too weak for use in the Merrill Tunnel since the wire would break too frequently. This was probably caused by dust and small particles in the flow. The amplified voltage fluctuations caused by turbulent flow

were fed into both an oscilloscope and an r.m.s. voltmeter. The transition from laminar to turbulent flow could be detected by reference to either of these two instruments. When turbulence first begins the r.m.s. voltage increases and finally reaches a peak when turbulence is complete. After complete turbulence is obtained the voltage drops off again. A plot of this voltage will determine the transitional region with very good accuracy. Since turbulence is a non-periodic phenomenon, the r.m.s. voltage fluctuates and reasonable care must be taken to determine the average value. The determination of transition by reference to the oscilloscope affords a very rapid method of detecting the transition region since this method requires only a visual interpretation of scope presentation. A representation of the type of agreement which may be obtained by use of the r.m.s. voltmeter and oscilloscope is shown in Figure 8. Since the use of an oscilloscope affords both an accurate and rapid method for determining the transition region, it was used to obtain the data reported herein.

Since the flow over the entire model at the lower tunnel velocities was laminar, a trip wire was used to induce transition. A 30 gauge bare copper wire ring was used on the nose section of the model 4 inches from the leading edge.

The data were obtained by placing the hot wire at a particular X/L position. As the tunnel velocity was increased the first indication of turbulence on the oscilloscope was recorded as the beginning of transition. The tunnel velocity was then increased until complete turbulence, or transition was indicated on the oscilloscope and this point was also recorded. The data were taken in this manner rather

than locating the transition region at constant velocity by traversing the hot wire, since it was found that the latter method was more difficult. The reason for this is discussed in Section IV.

The above procedure was repeated at many stations along the model for angles of yaw of 0, 5, and 10 degrees and rates of spin of 0, $\pm$ 5 and $\pm$ 10 revolutions per second. Most of the data were taken on the lower side of the model, the yaw plane being horizontal. Complete data were not obtained in all cases because of two primary difficulties encountered. At the higher tunnel velocities it was found that the model vibrated a considerable amount as a result of excitation of natural frequency modes in the supporting structure. Due to dynamic unbalance, vibrations also occurred at spin rates in excess of 10 revolutions per second. These vibrations induced velocity fluctuations which could be detected with the hot wire at zero free stream velocity. Neither of these two difficulties could be eliminated during the course of this investigation.

IV. DISCUSSION OF RESULTS

The tuft studies give no indication as to whether the boundary layer flow is laminar or turbulent; however, some indication as to the general nature of the flow about the body is given. The tuft patterns, shown in Figures 4 through 7, suggest that at angles of yaw above five degrees vortices are generated on the leeward side of the model. Later studies made with the hot wire indicated that no nonstationary vortices were generated at a five degree yaw angle. However, velocity fluctuations occurred in the laminar layer immediately prior to transition, and complete transition occurred at a lower Reynolds number than on the lower side.

It is believed that the tuft vibrations were caused by the material properties of the tufts rather than turbulence.

The data obtained on the lower side of the model by use of the hot wire are presented in the form of Re_x, for both beginning and completion of transition, plotted versus X/L positions along the model in Figures 9 through 21. As shown in these figures such a plot forms straight lines, except near the nose section for zero spin. The Re_x for both beginning and completion of transition from laminar to turbulent flow is much higher near the nose section for the case of zero spin. The cause of this "hump" was not completely determined; however, in an effort to determine if this was caused by the tripping device, data were taken with the trip wire moved four inches downstream, or eight inches from the nose. It was found that the "hump" did not move appreciably. In Figure 9 there are shown lines of constant velocity. As may be seen from this figure, only a small velocity increase is required to change the boundary layer flow over the entire length of the

model from laminar to turbulent, excluding the nose section. This explains why the data could be obtained more easily at constant X/L positions rather than at constant velocities, since a small change in velocity would cause a large shift of the transition region. Figure 9 also shows that for all practical purposes the boundary layer flow is either completely laminar or completely turbulent, since the lines of constant velocity and transition Reynolds numbers intersect at very small angles. It will be noted that data are not presented for the entire length of the model in all cases. Data were not taken in these cases due to the difficulties outlined in Section III.

The data for complete transition and zero spin are replotted as Re_x vs. Re_d in Figures 22 through 24. This type of plot is essentially velocity of transition vs. Re_x. Figure 22 shows that, for the case of zero spin and yaw, transition occurs at a fixed Re_x over the nose section and at an almost constant Re_d downstream of the nose section. This is essentially the same type of result obtained with a flat plate having a tripping device at supersonic speeds as reported in reference 7.

The results obtained would also be true for the upper surface and may be discussed in three groups as follows:

1. Effect of Yaw

Reference to Figures 9, 10, and 11 shows that an increase in angle of yaw increases the Re_x of both beginning and completion of transition over most of the model downstream of the nose section. Figure 25 shows Re_x for complete transition plotted versus yaw angle for several X/L positions along the model. To obtain this figure, points were extrapolated for the case of ten degrees yaw by extending

the complete transition Re_x line to the larger X/L values. It is reasonable to assume that this line would be straight since this was true for all cases where data could be obtained. Based on this assumption, Figure 25 shows that for smaller values of X/L and at smaller angles of yaw there is a possible reversal of the effect of yaw, that is, for these regions increasing angle of yaw decreases the transition Re_x. This effect is, however, extremely small. It may also be seen that the increase in Re_x is larger than the trigonometric relationship of the angles involved; that is, transition occurs at a higher axial velocity when the model is in a yawed position. As shown in Figures 22 through 24 an increase in angle of yaw tends to cause complete transition to occur along lines of smaller X but at larger values of both Re_d and Re_x. This means that transition occurs nearer the nose section but at a higher velocity.

2. Effect of Spin

Figure 26 shows the Re_x of complete transition replotted versus spin rate with zero yaw for several X/L positions along the model. It will be noted from this figure that the general effect of spin is to decrease the Re_x for transition; although a reversal in this effect is indicated for the smaller spin rate at the smaller X/L positions. Again this reversal is of small magnitude. Figure 4 of reference 8 shows that the effect of spin, if any, is to move the transition region rearward. The reference report covers the region which would correspond to an X/L of less than 0.4 for the model used in this investigation and therefore a direct comparison of the results obtained may not be valid. A secondary effect of spin, which may be observed from the figures, is

to increase the width of the transition region.

3. Combined Effect of Spin and Yaw

Figure 27 shows the effects of the various rates of spin for a yaw angle of five degrees compared to the values obtained at zero yaw and spin for several X/L values. As shown by this figure, the Re_x for complete transition is lower with spin and yaw than at zero spin and yaw. There is no noticeable difference in the results obtained with the two directions of spin. As before, a reversal of this effect is indicated at the smaller X/L and spin rate values. The overall effect of combined spin and yaw is very small. Considering the fact that spin alone has a negligible effect on transition, and that yaw alone has a rather large effect; it is indicated that the combined effect of spin and yaw is dominated by spin.

V. CONCLUSIONS

Since the transition region is of such nature that it can not be clearly defined and since the effects of spin and yaw observed in this investigation were small, very few definite conclusions can be made.

The following trends were observed to be true for the body of revolution studied and are presented in hope that they may be of value to those who might further investigate this subject:

1. There is no unique transition Reynolds number for the entire body, the Reynolds number of transition being different on different portions of the body.
2. The boundary layer flow for all practical purposes is either completely laminar or completely turbulent.
3. The effect of spin on boundary layer transition is negligible.
4. The transition Reynolds number is increased on the upper and lower surfaces by an angle of yaw. At angles of yaw transition occurs at a lower Reynolds number on the leeward side than on the upper and lower surfaces.

REFERENCES

1. Merrill Wind Tunnel Calibration Report, Aeronautics Library, California Institute of Technology.

2. Stalder, Jackson R. and Slack, Ellis G., "The Use of a Luminescent Lacquer for the Visual Indication of Boundary-Layer Transition", NACA TN 2263, (January 1951).

3. Koone, David S., "Determination of the Boundary Layer Transition by Means of a Flourescant Lacquer", Report for the Hypersonic Wind Tunnel, California Institute of Technology, (May 23, 1952).

4. "Review of Hot Wire Anemometry", Australian Council for Aeronautics, Report ACA-19, (October, 1945).

5. Kovasznay, Laszo, "Calibration and Measurement in Turbulence Research by the Hot Wire Method", NACA TM 1130, (June 1947).

6. Schubauer, G. B. and Klebnoft, P. S., "Theory and Application of Hot Wire Instruments in the Investigation of Turbulent Boundary Layers", NACA ACR 5N27, (March, 1946).

7. Coles, Donald, "Measurements in the Boundary Layer on a Smooth Flat Plate in Supersonic Flow", JPL Report 20-17, California Institute of Technology, (June 1953).

8. Schmidt, L. E. and Murphy, C. H., "Effect of Spin on Aerodynamic Properties of Bodies of Revolution", Ballistic Research Laboratories Memorandum Report 715, (August 1952).

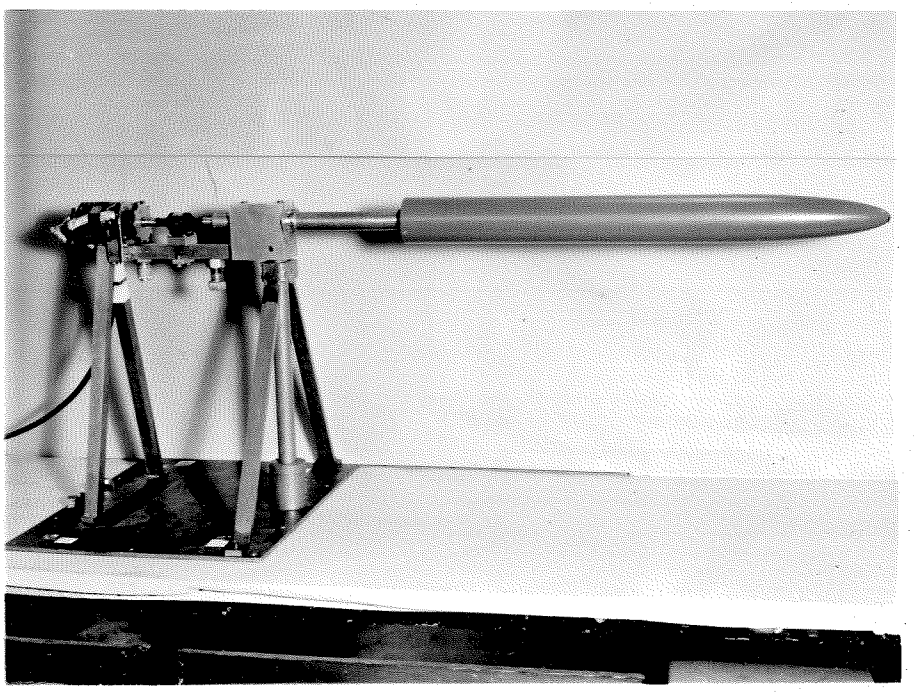

FIGURE 1

MODEL AND MOUNTING

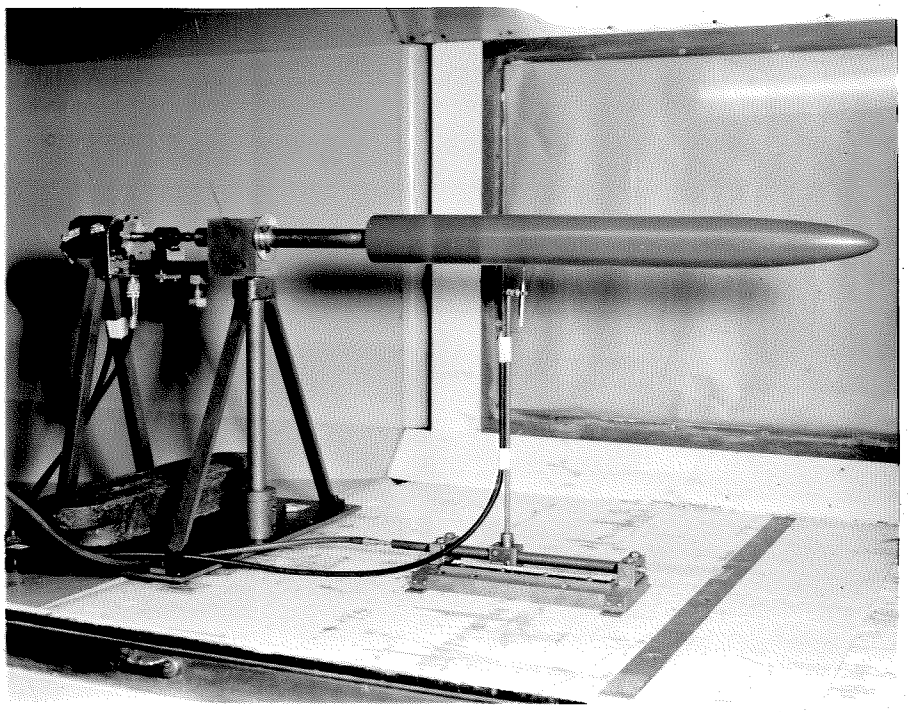

FIGURE 2

MODEL AND HOT WIRE INSTALLATION

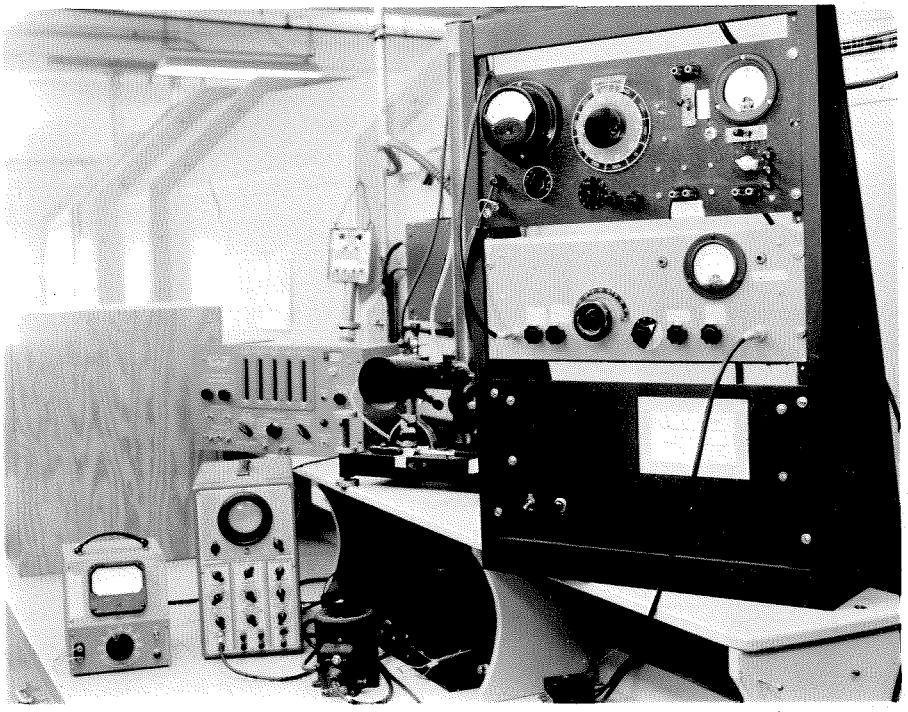

FIGURE 3

AUXILIARY EQUIPMENT

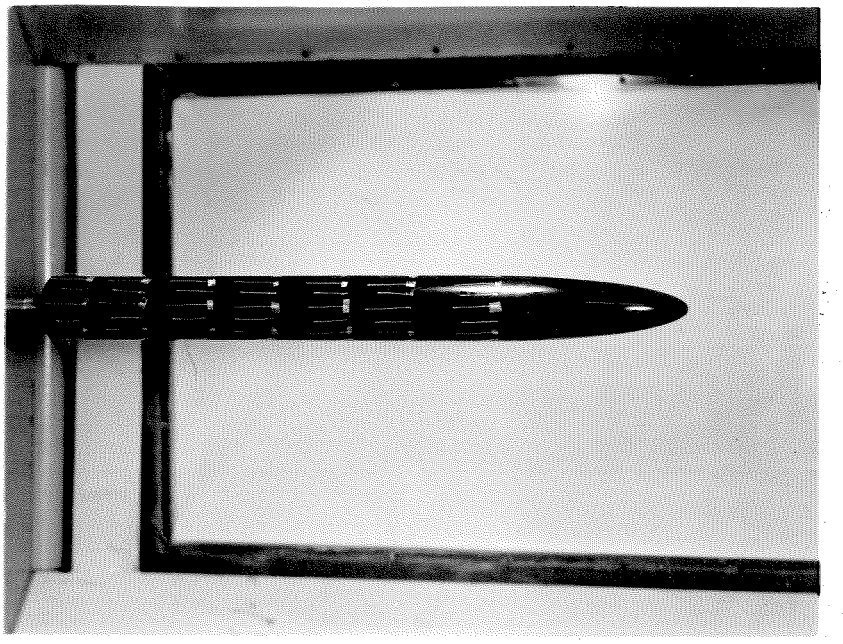

(a) Air Speed 9.1 ft./sec.

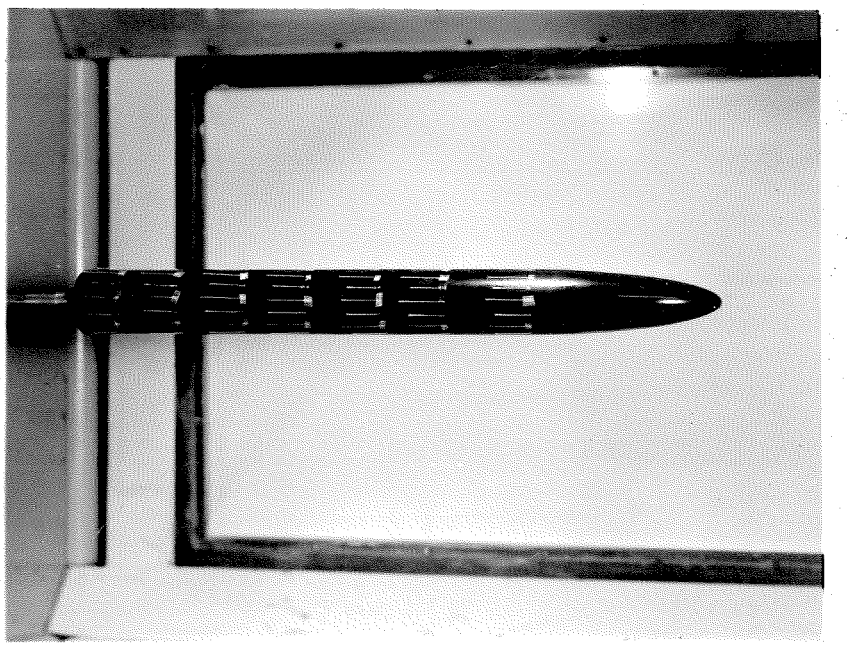

(b) Air Speed 154 ft./sec.

FIGURE 4

TUFT FORMATIONS ON MODEL AT ZERO YAW

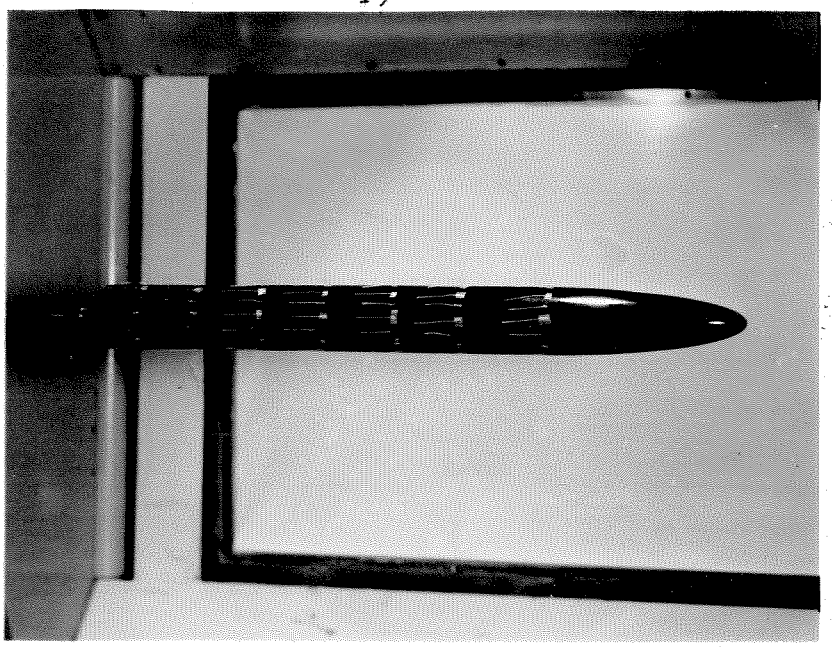

(a) Air Speed 9.6 ft./sec.

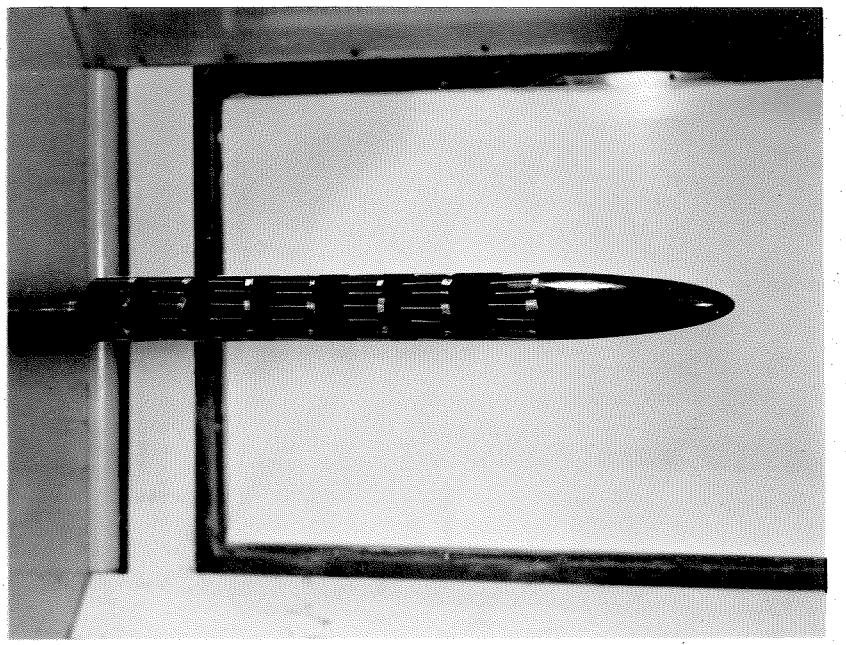

(b) Air Speed 153 ft./sec.

FIGURE 5

TUFT FORMATIONS ON LEE SIDE OF MODEL

FIVE DEGREES YAW

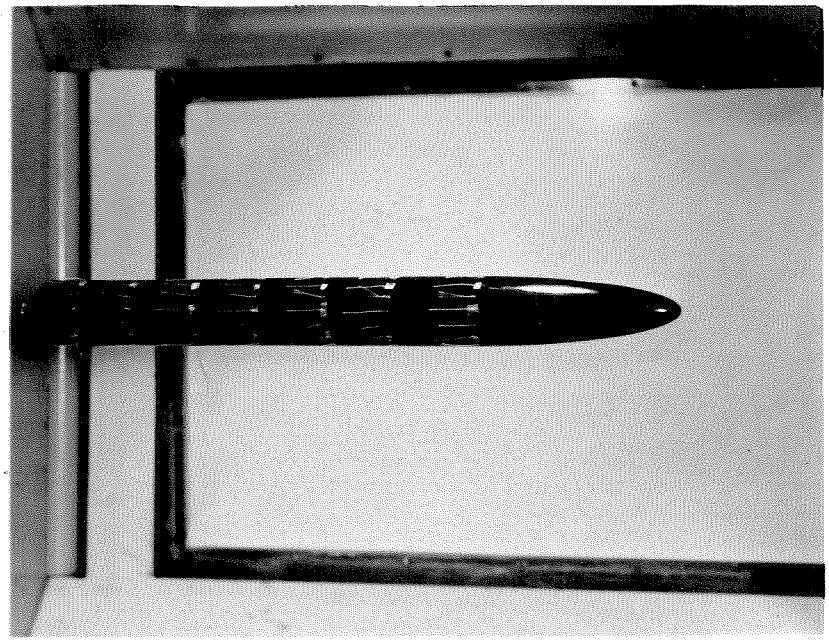

(a) Air Speed 9.7 ft./sec.

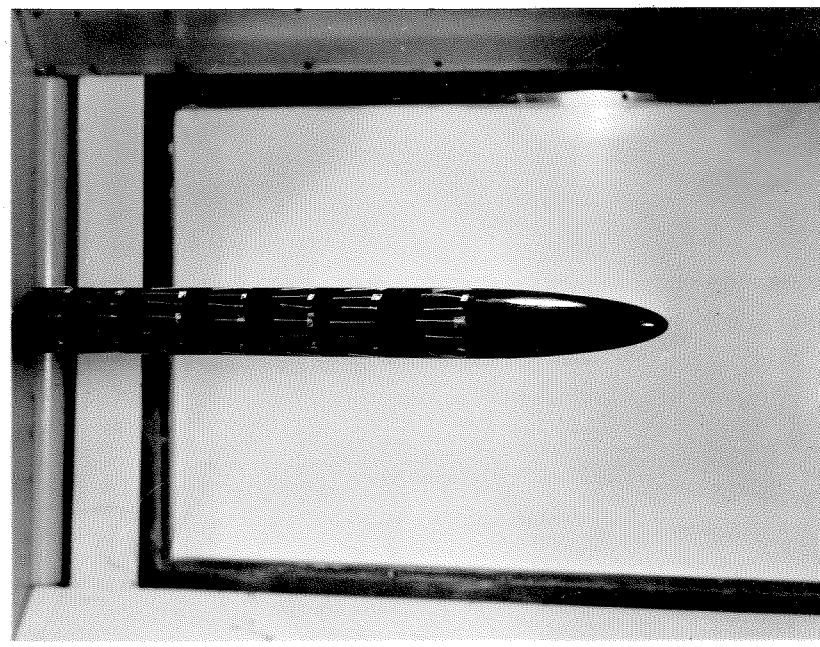

(b) Air Speed 154 ft./sec.

FIGURE 6

TUFT FORMATIONS ON LEE SIDE OF MODEL

TEN DEGREES YAW

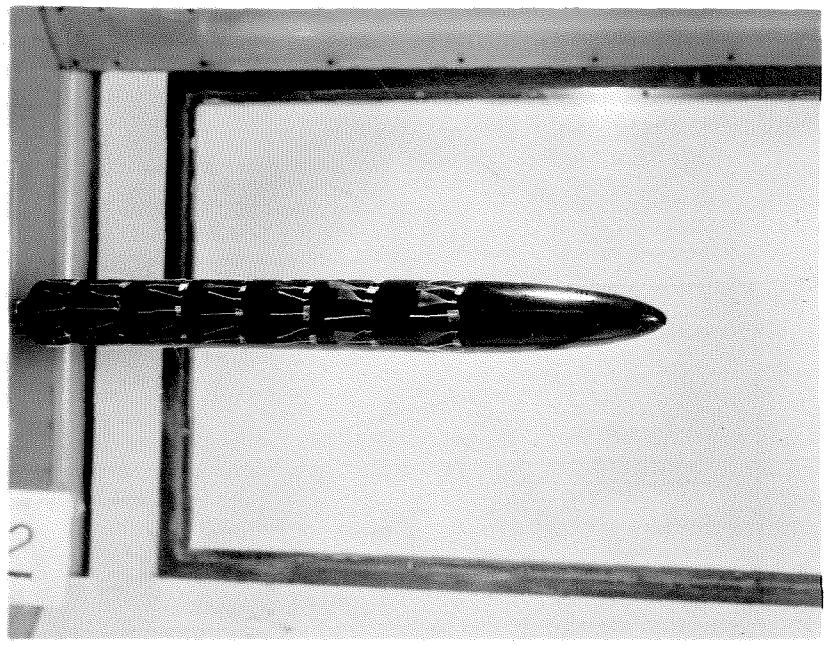

(a) Air Speed 9.5 ft./sec.

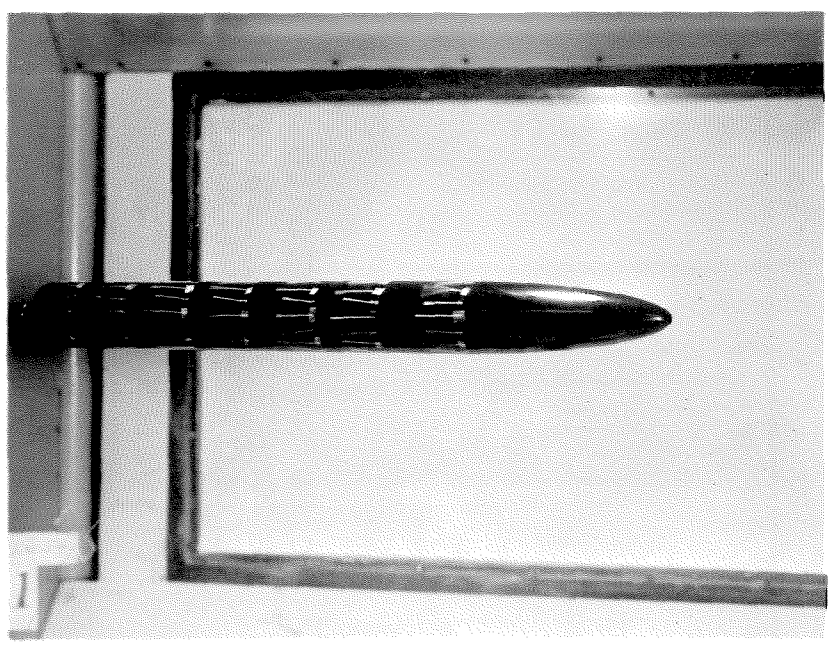

(b) Air Speed 150 ft./sec.

FIGURE 7

TUFT FORMATIONS ON LEE SIDE OF MODEL

FIFTEEN DEGREES YAW

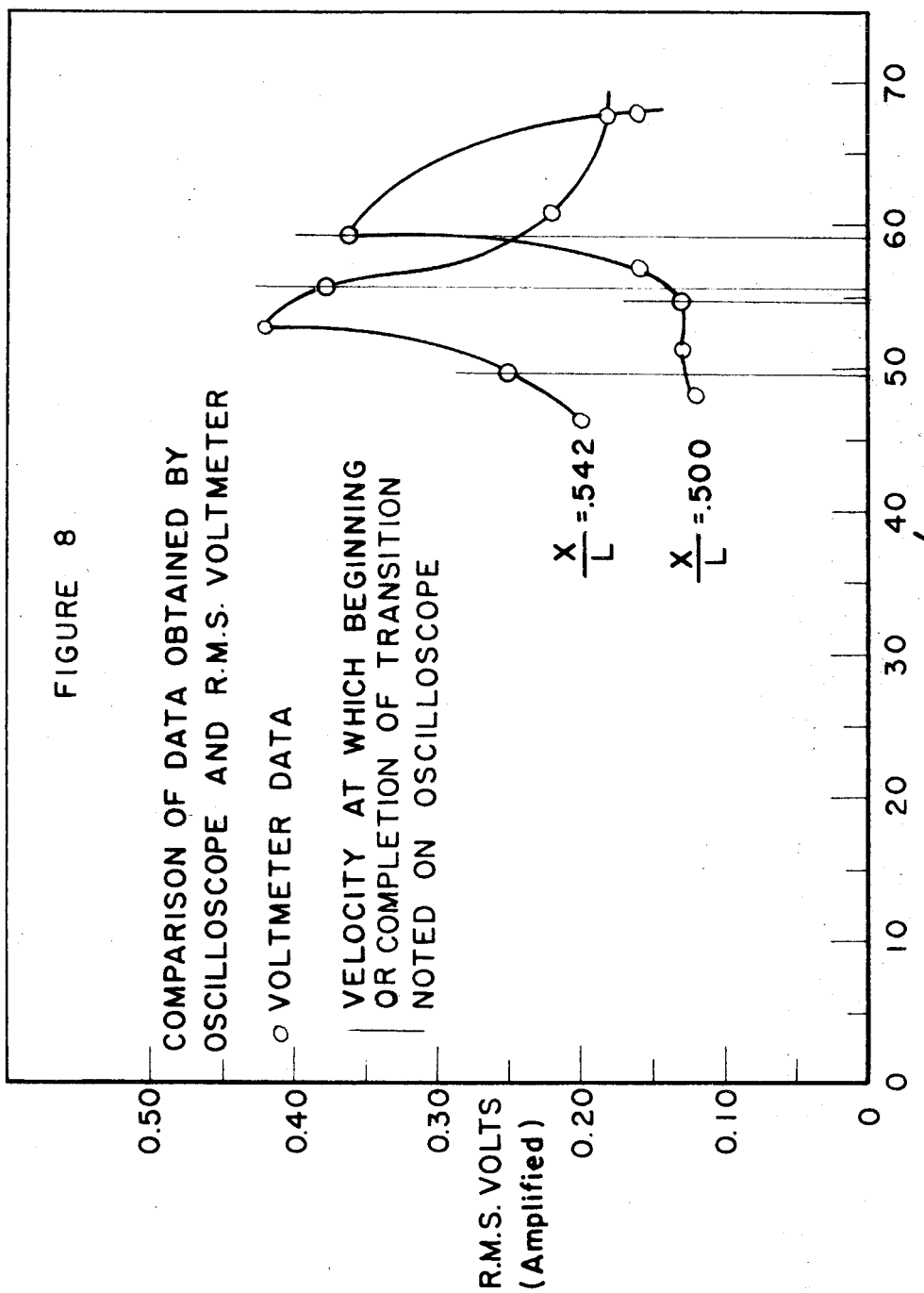
FIGURE 8
COMPARISON OF DATA OBTAINED BY
OSCILLOSCOPE AND R.M.S. VOLTMETER
○ VOLTMETER DATA
| VELOCITY AT WHICH BEGINNING
OR COMPLETION OF TRANSITION
NOTED ON OSCILLOSCOPE
X/L = .542
X/L = .500
R.M.S. VOLTS
(Amplified)
0.50
0.40
0.30
0.20
0.10
0
0
10
20
30
40
50
60
70
u, ft/sec

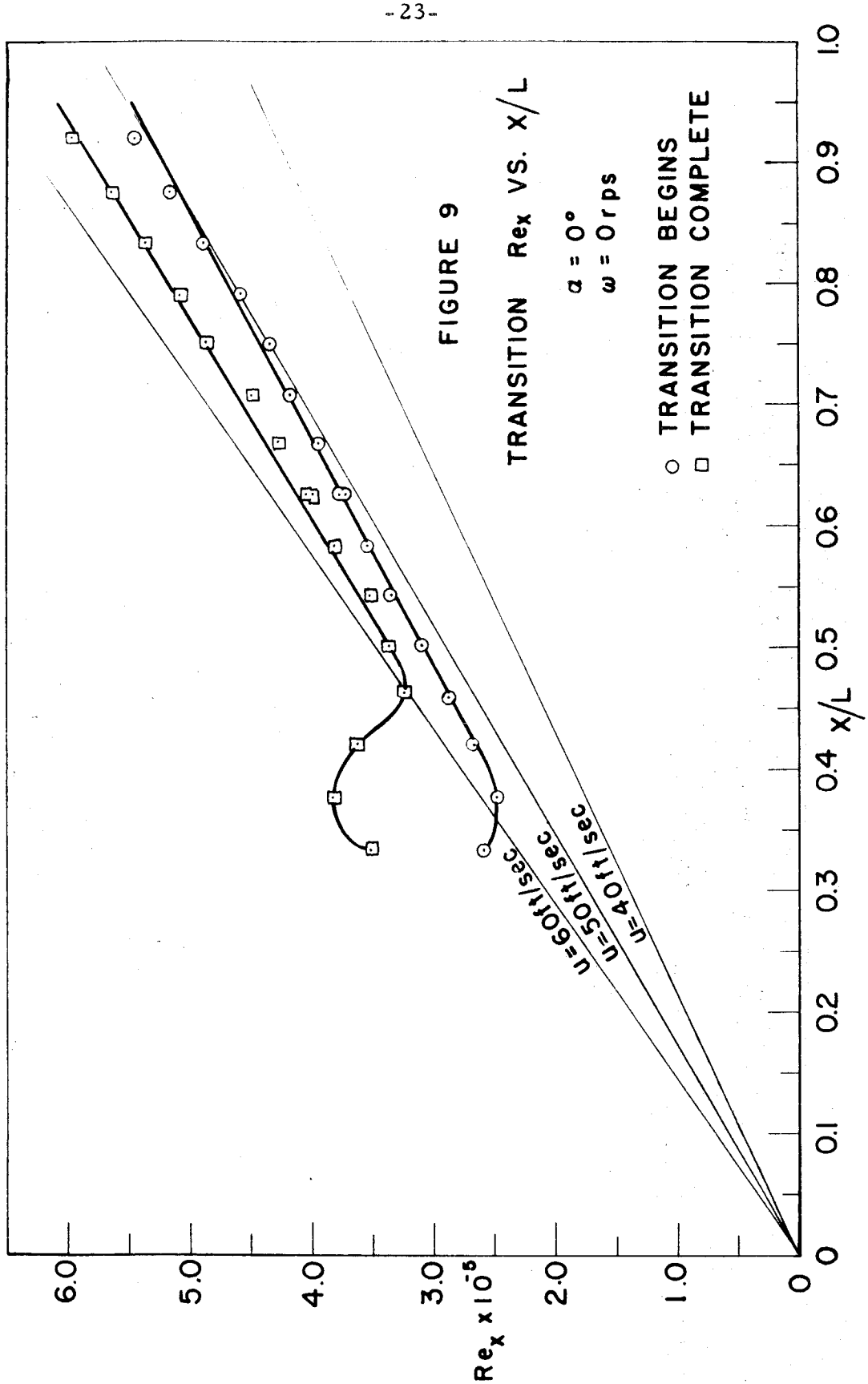
FIGURE 9
TRANSITION Re_x VS. X/L
$\alpha = 0°$
$\omega = 0$ rps
○ TRANSITION BEGINS
□ TRANSITION COMPLETE
U=60ft/sec
U=50ft/sec
U=40ft/sec
$Re_x \times 10^{-5}$
X/L
0
0.1
0.2
0.3
0.4
0.5
0.6
0.7
0.8
0.9
1.0
1.0
2.0
3.0
4.0
5.0
6.0

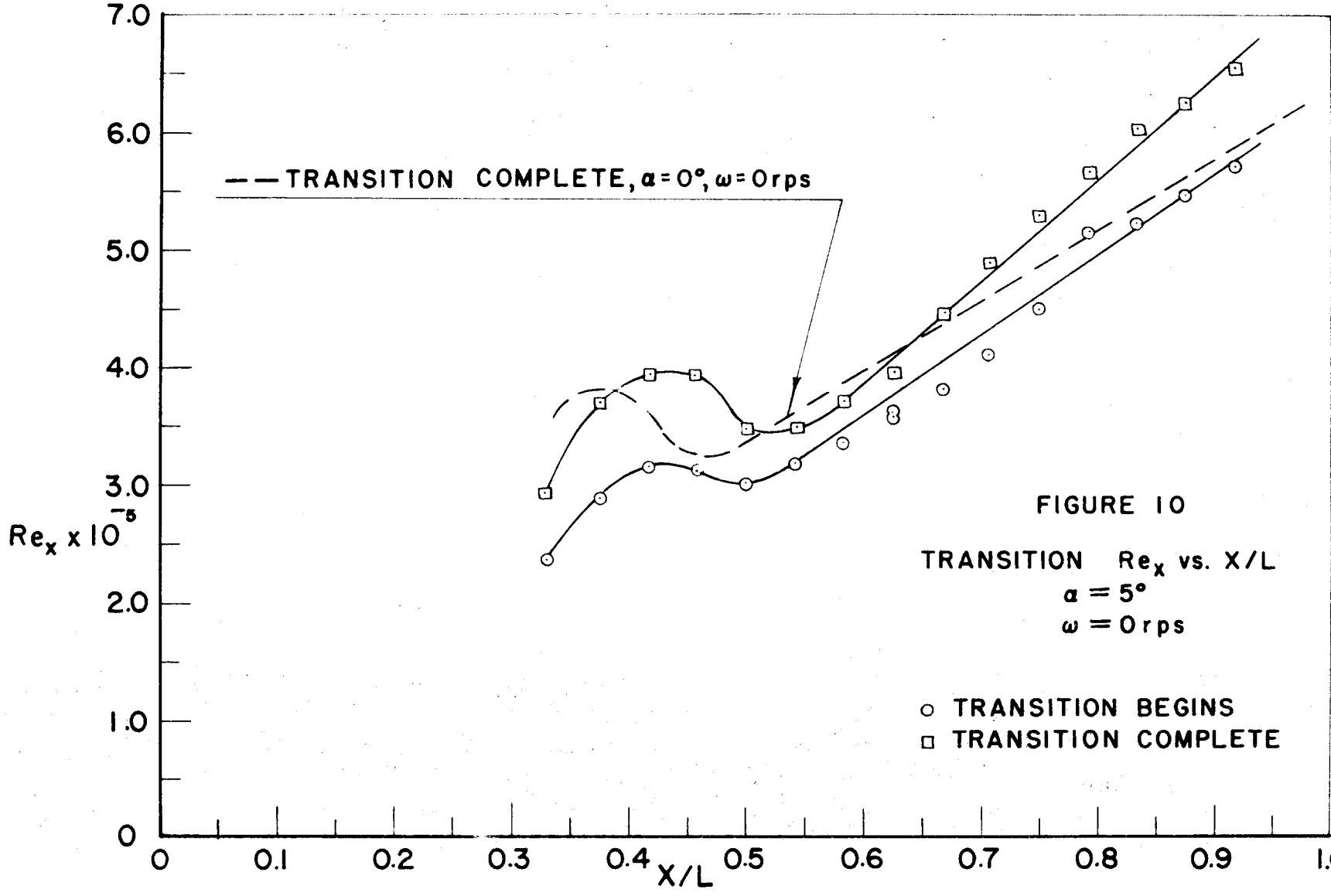
7.0
6.0
5.0
4.0
3.0
2.0
1.0
0
$Re_x \times 10^{-5}$
0
0.1
0.2
0.3
0.4
X/L
0.5
0.6
0.7
0.8
0.9
1.0
— — TRANSITION COMPLETE, α = 0°, ω = 0 rps
FIGURE 10
TRANSITION Re_x vs. X/L
α = 5°
ω = 0 rps
○ TRANSITION BEGINS
□ TRANSITION COMPLETE

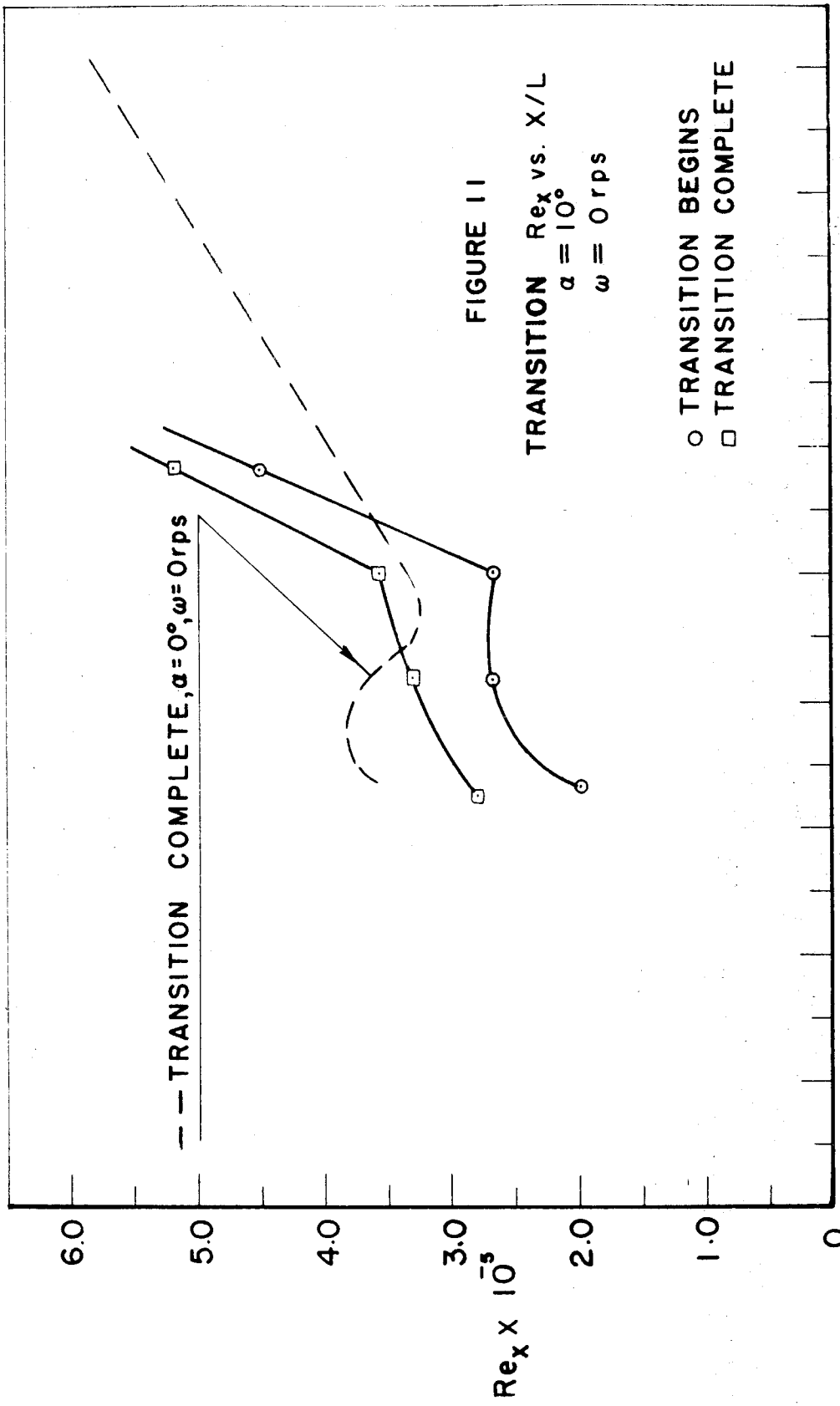
FIGURE 11
TRANSITION Re_x vs. X/L
α = 10°
ω = 0 rps
○ TRANSITION BEGINS
□ TRANSITION COMPLETE
— — TRANSITION COMPLETE, α = 0°, ω = 0 rps
$Re_x \times 10^{-5}$
X/L
0
0.1
0.2
0.3
0.4
0.5
0.6
0.7
0.8
0.9
1.0
2.0
3.0
4.0
5.0
6.0

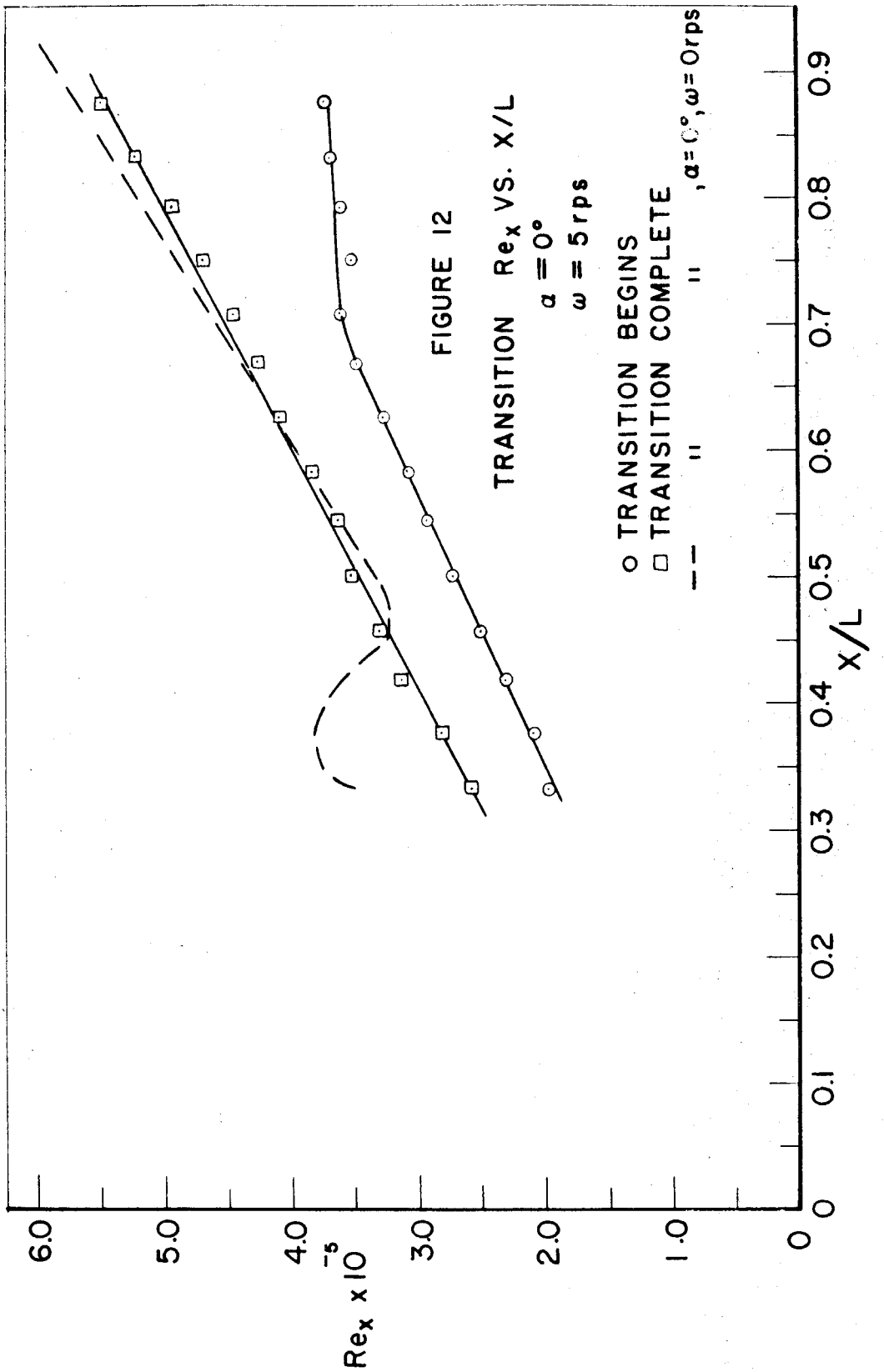
FIGURE 12
TRANSITION Re_x VS. X/L
$\alpha = 0°$
$\omega = 5$ rps
o TRANSITION BEGINS
□ TRANSITION COMPLETE
— — " " , $\alpha = 0°, \omega = 0$ rps
$Re_x \times 10^{-5}$
X/L
0
0.1
0.2
0.3
0.4
0.5
0.6
0.7
0.8
0.9
1.0
2.0
3.0
4.0
5.0
6.0

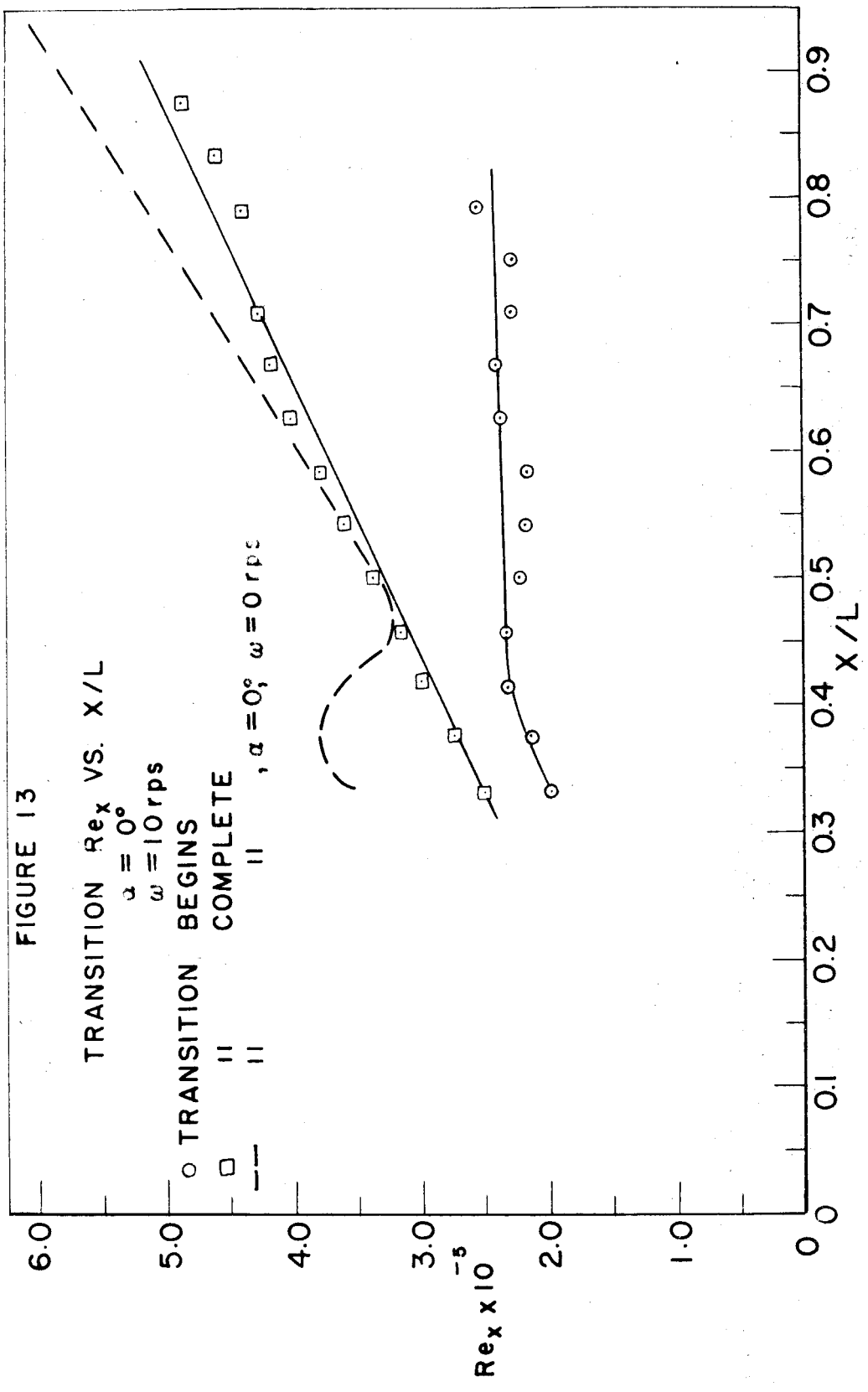
FIGURE 13
TRANSITION Re_x VS. X/L
$\alpha = 0°$
$\omega = 10$ rps
○ TRANSITION BEGINS
□ " COMPLETE
— — " , $\alpha = 0°$; $\omega = 0$ rps
$Re_x \times 10^{-5}$
X/L
0.0
0.1
0.2
0.3
0.4
0.5
0.6
0.7
0.8
0.9
1.0
2.0
3.0
4.0
5.0
6.0

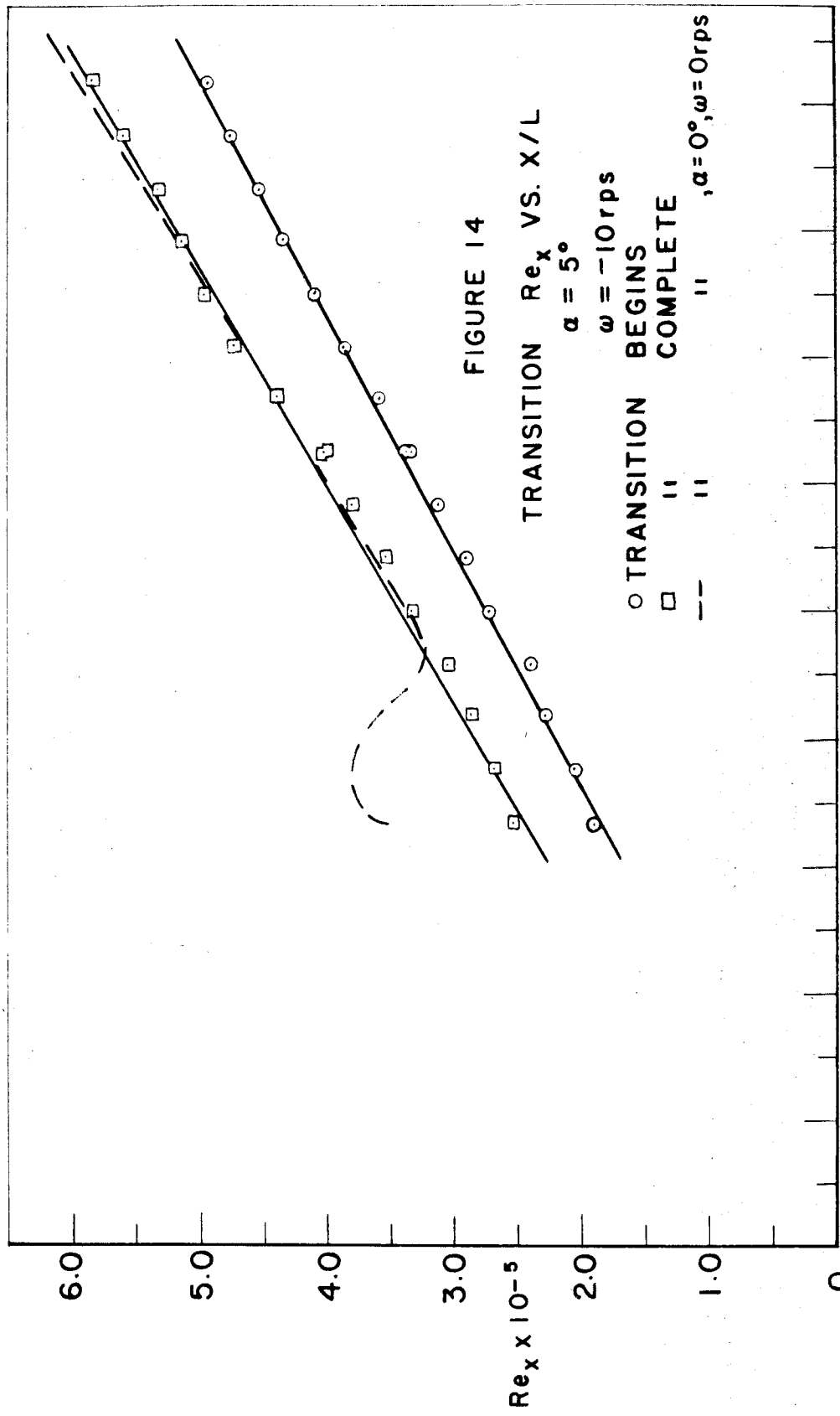
FIGURE 14
TRANSITION Re_x VS. X/L
$\alpha = 5°$
$\omega = -10$ rps
○ TRANSITION BEGINS
□ " COMPLETE
— — " , $\alpha = 0°, \omega = 0$ rps
$Re_x \times 10^{-5}$
X/L
0
0.1
0.2
0.3
0.4
0.5
0.6
0.7
0.8
0.9
1.0
2.0
3.0
4.0
5.0
6.0

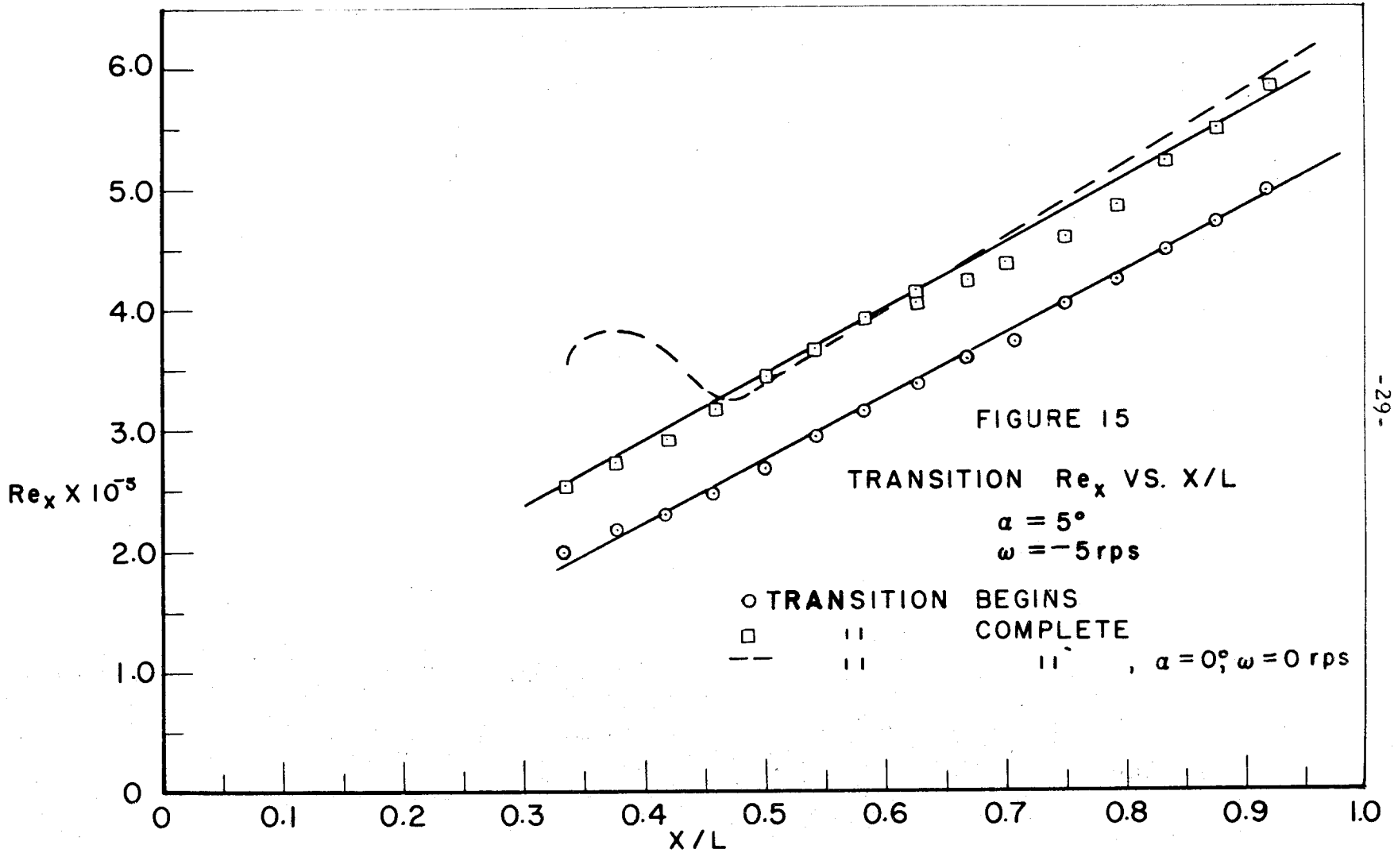
6.0
5.0
4.0
3.0
2.0
1.0
0
$Re_x \times 10^{-5}$
0
0.1
0.2
0.3
0.4
0.5
0.6
0.7
0.8
0.9
1.0
X/L
FIGURE 15
TRANSITION Re_x VS. X/L
$\alpha = 5°$
$\omega = -5$ rps
○ TRANSITION BEGINS
□ " COMPLETE
— — " " , $\alpha = 0°, \omega = 0$ rps

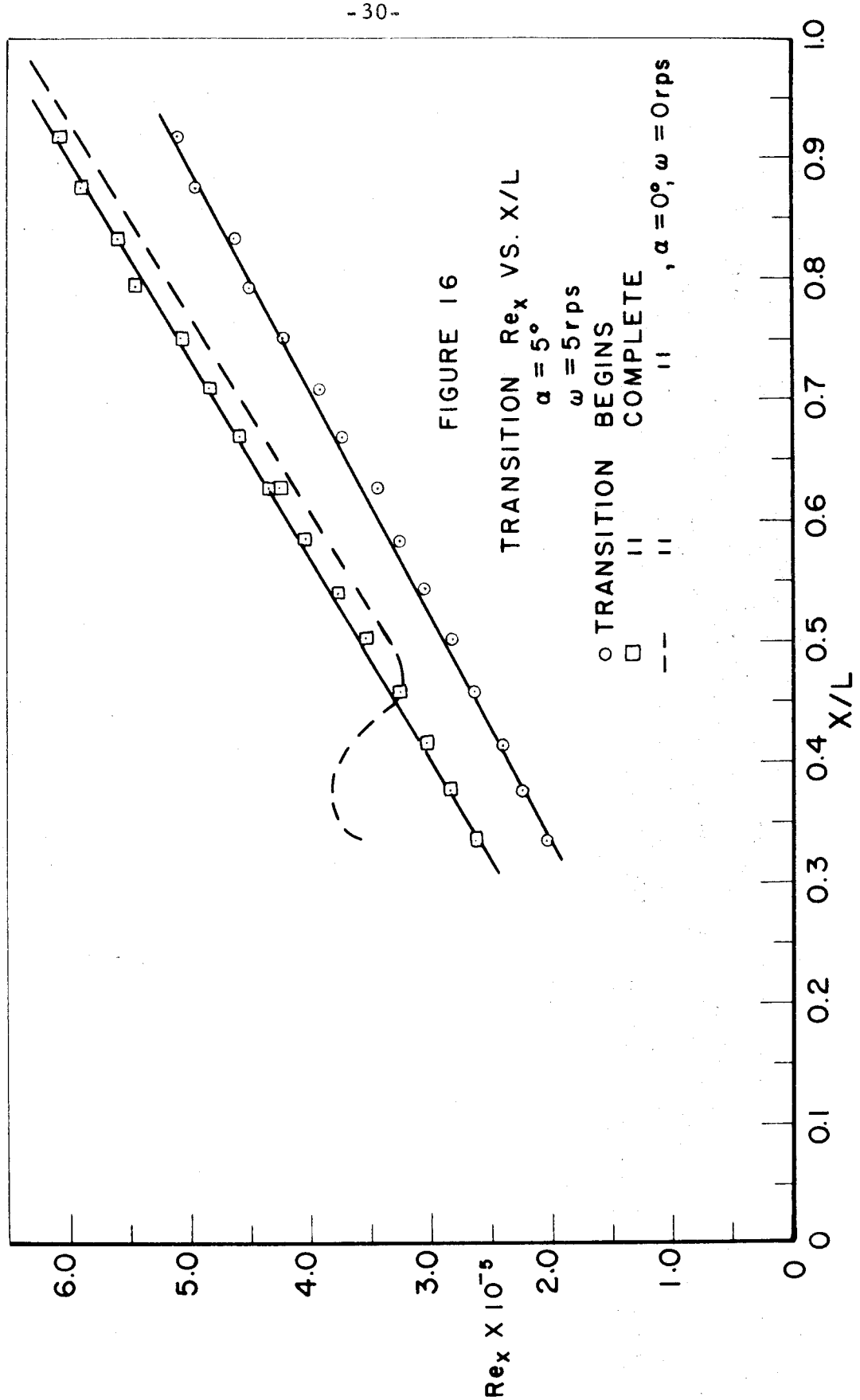
FIGURE 16
TRANSITION Re_x VS. X/L
$\alpha = 5°$
$\omega = 5$ rps
○ TRANSITION BEGINS
□ " COMPLETE
— — " , $\alpha = 0°$, $\omega = 0$ rps
$Re_x \times 10^{-5}$
X/L
0
0.1
0.2
0.3
0.4
0.5
0.6
0.7
0.8
0.9
1.0
1.0
2.0
3.0
4.0
5.0
6.0

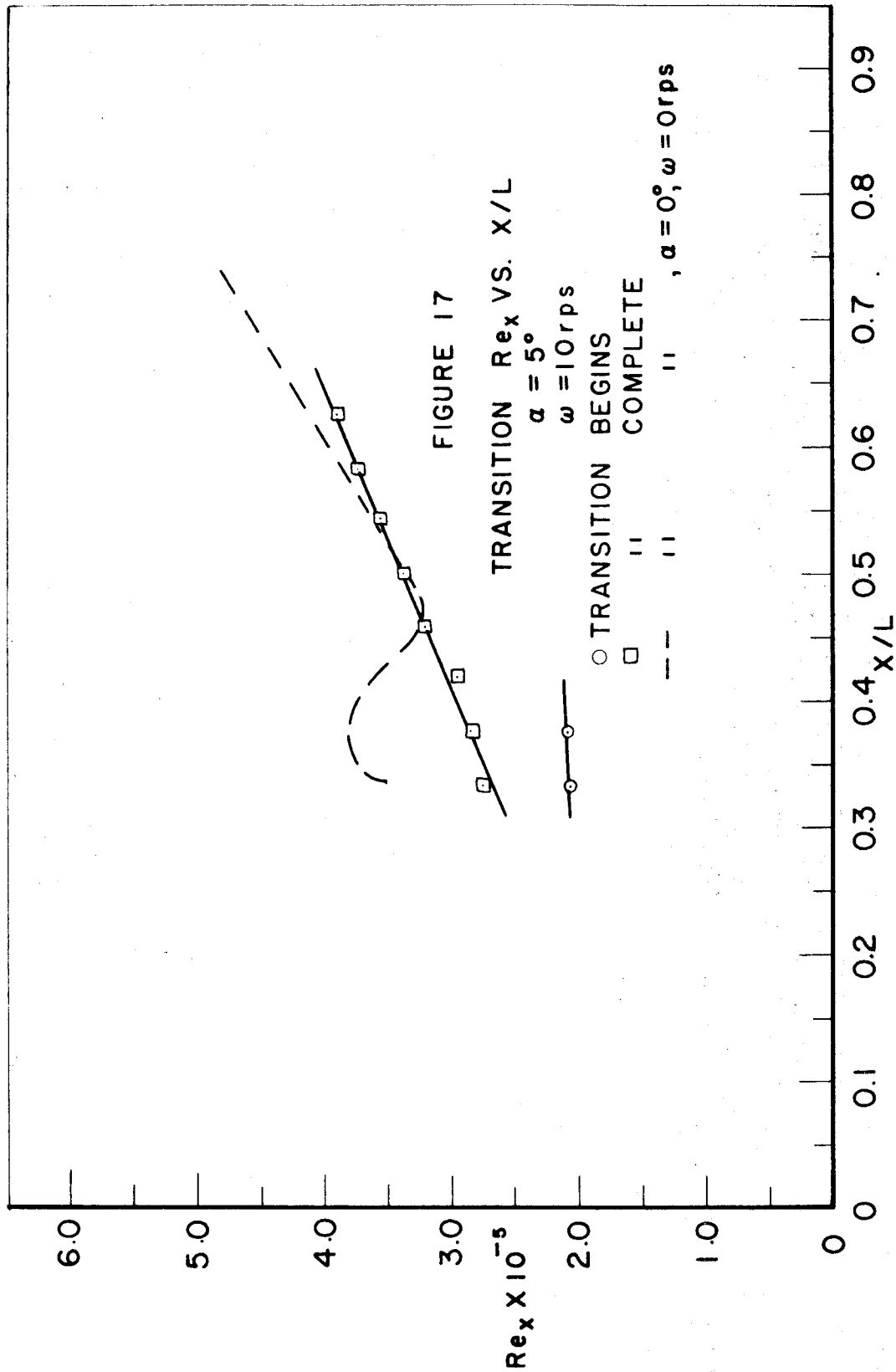
FIGURE 17
TRANSITION Re_x VS. X/L
$\alpha = 5°$
$\omega = 10$ rps
○ TRANSITION BEGINS
□ " COMPLETE
— — " " , $\alpha = 0°$, $\omega = 0$ rps
$Re_x \times 10^{-5}$
6.0
5.0
4.0
3.0
2.0
1.0
0
0.1
0.2
0.3
0.4
X/L
0.5
0.6
0.7
0.8
0.9

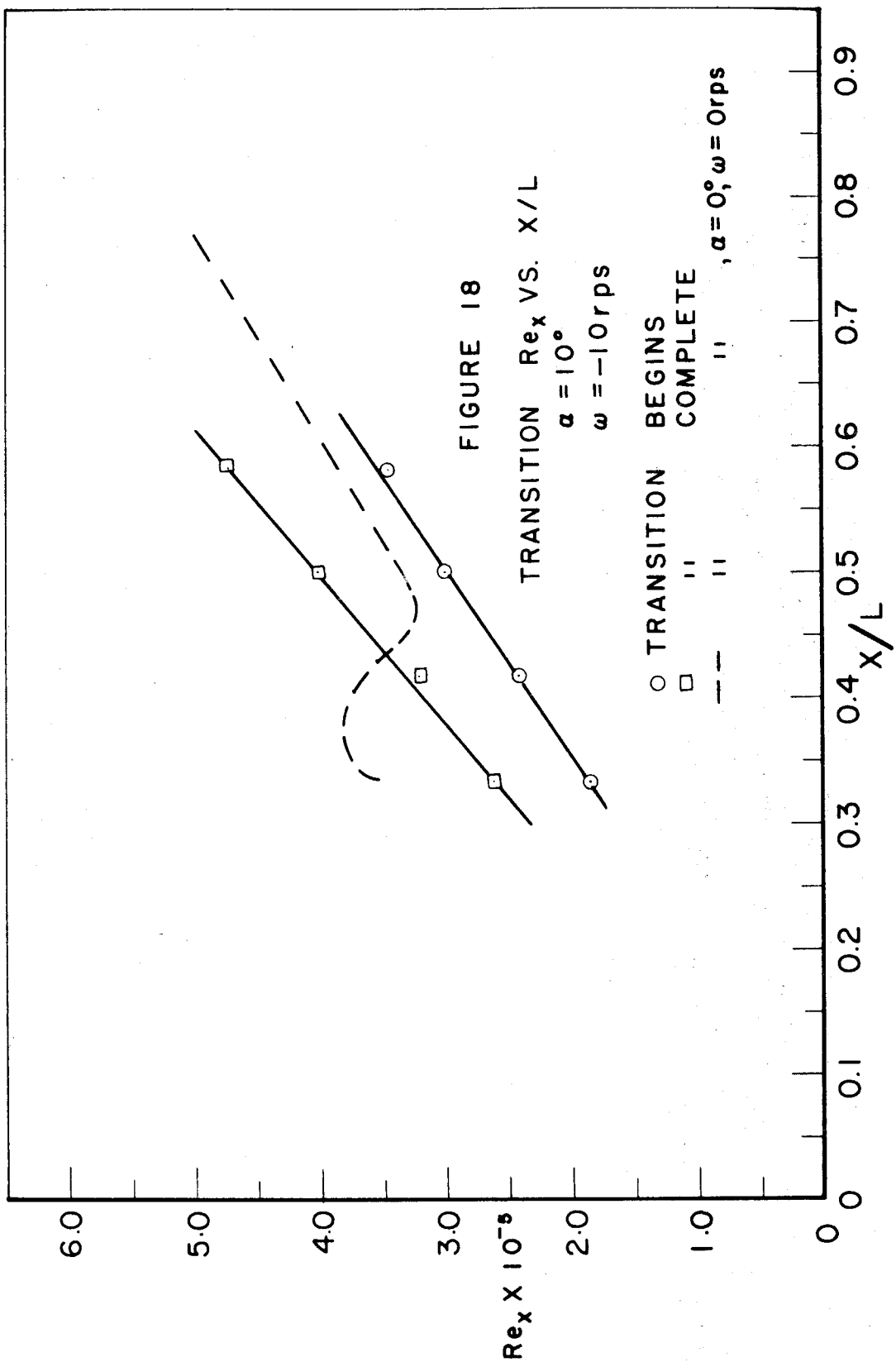
FIGURE 18
TRANSITION Re_x VS. X/L
$\alpha = 10°$
$\omega = -10$ rps
○ TRANSITION BEGINS
□ " COMPLETE
— — " , $\alpha = 0°; \omega = 0$ rps
$Re_x \times 10^{-5}$
X/L
0
0.1
0.2
0.3
0.4
0.5
0.6
0.7
0.8
0.9
1.0
2.0
3.0
4.0
5.0
6.0

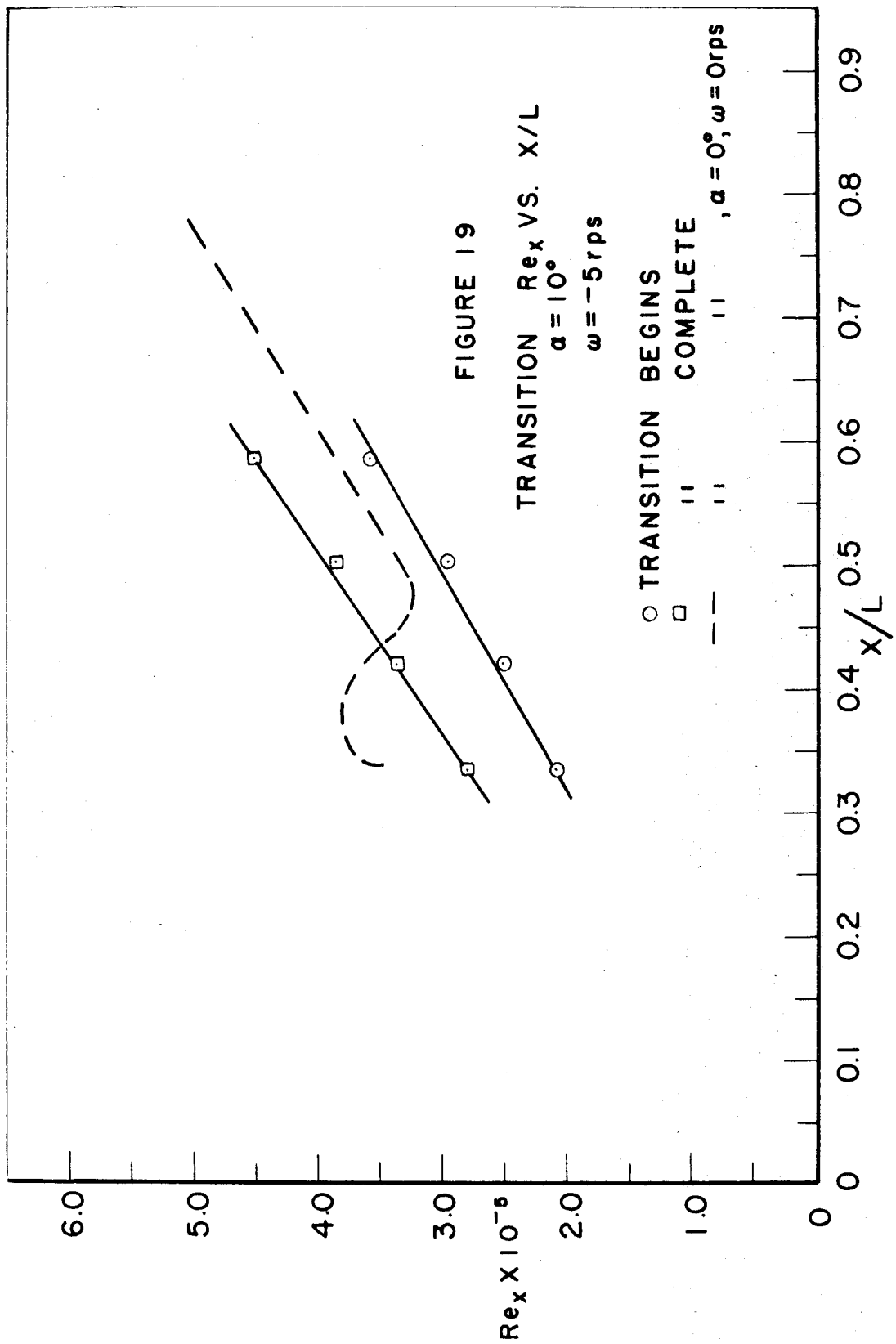
FIGURE 19
TRANSITION Re_x VS. X/L
$\alpha = 10°$
$\omega = -5$ rps
○ TRANSITION BEGINS
□ " COMPLETE
— — " , $\alpha = 0°, \omega = 0$ rps
$Re_x \times 10^{-5}$
6.0
5.0
4.0
3.0
2.0
1.0
0
0.1
0.2
0.3
0.4
X/L
0.5
0.6
0.7
0.8
0.9

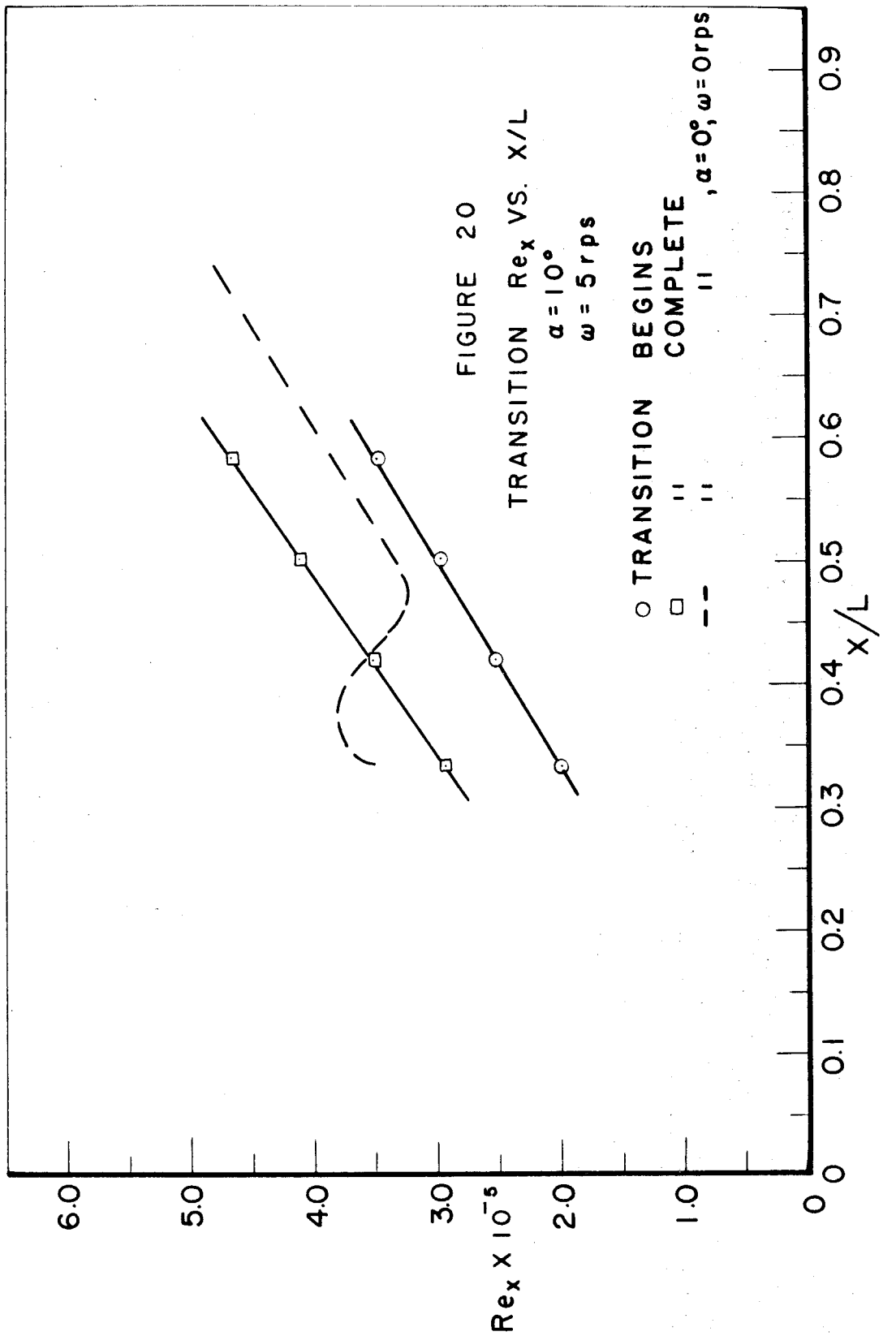
FIGURE 20
TRANSITION Re_x VS. X/L
$\alpha = 10°$
$\omega = 5$ rps
○ TRANSITION BEGINS
□ " COMPLETE
— — " , $\alpha = 0°$; $\omega = 0$ rps
$Re_x \times 10^{-5}$
X/L
0
0.1
0.2
0.3
0.4
0.5
0.6
0.7
0.8
0.9
1.0
2.0
3.0
4.0
5.0
6.0

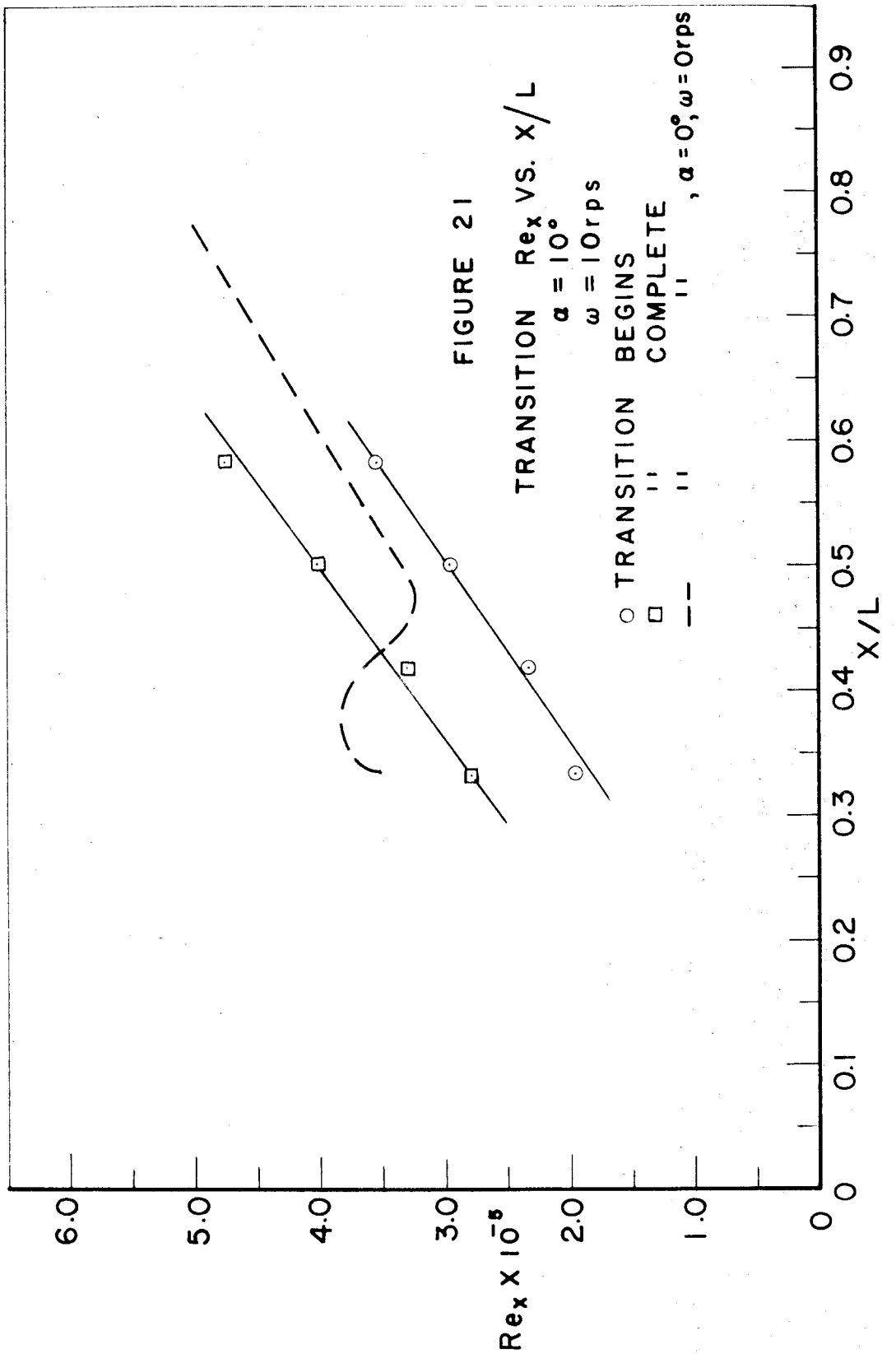
FIGURE 21
TRANSITION Re_x VS. X/L
$\alpha = 10°$
$\omega = 10$ rps
○ TRANSITION BEGINS
□ " COMPLETE
— — " , $\alpha = 0°, \omega = 0$ rps
$Re_x \times 10^{-5}$
X/L
0
0.1
0.2
0.3
0.4
0.5
0.6
0.7
0.8
0.9
1.0
2.0
3.0
4.0
5.0
6.0

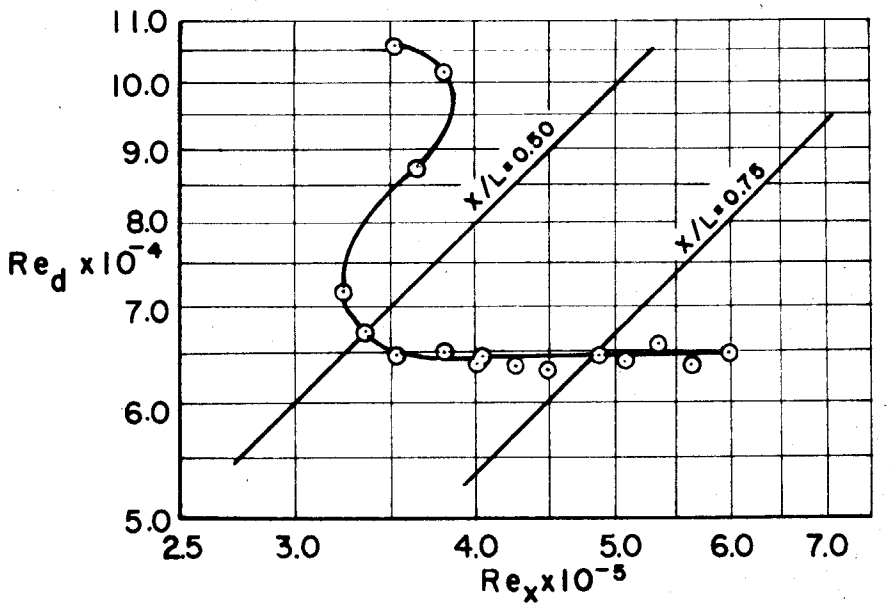

FIGURE 22

Re_d vs. Re_x FOR COMPLETE TRANSITION

$\alpha = 0°$

$\omega = 0$ rps

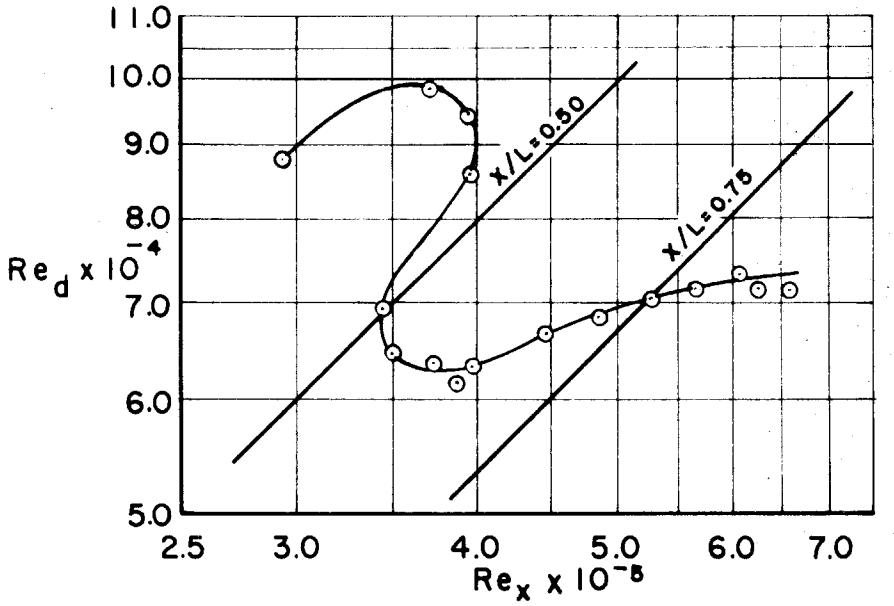

FIGURE 23

Re_d vs. Re_x FOR COMPLETE TRANSITION

$\alpha = 5°$

$\omega = 0$ rps

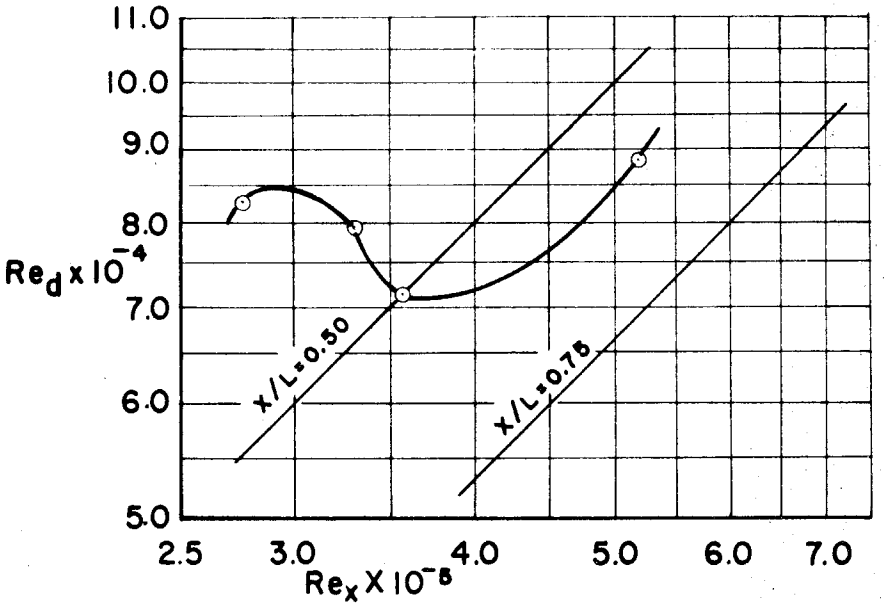

FIGURE 24

Re_d vs. Re_x FOR COMPLETE TRANSITION

$\alpha = 10°$

$\omega = 0$ rps

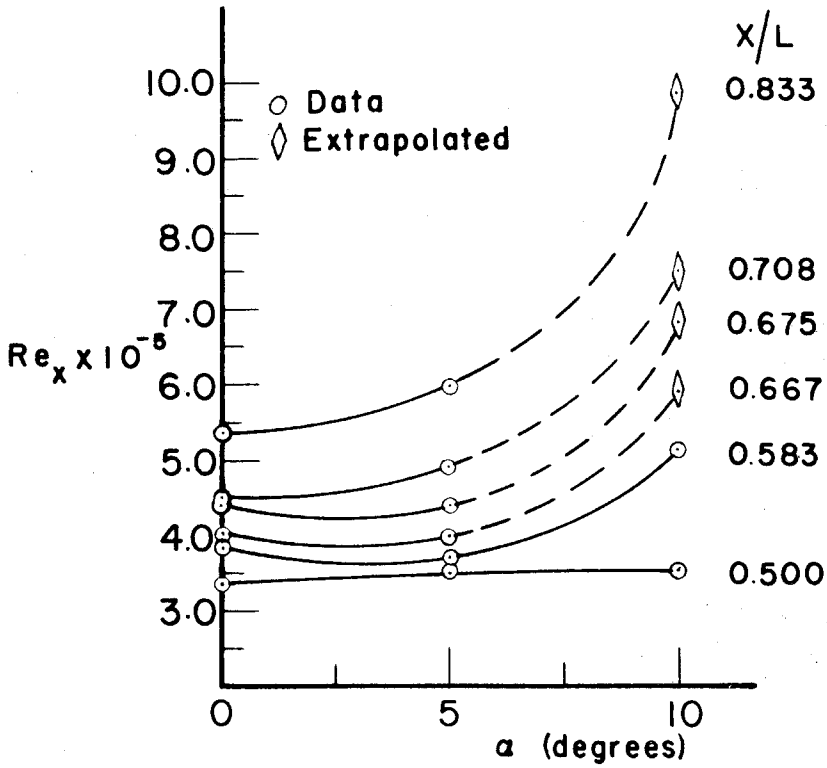

FIGURE 25
Re_x vs. YAW ANGLE FOR COMPLETE TRANSITION
$\omega = 0$ rps

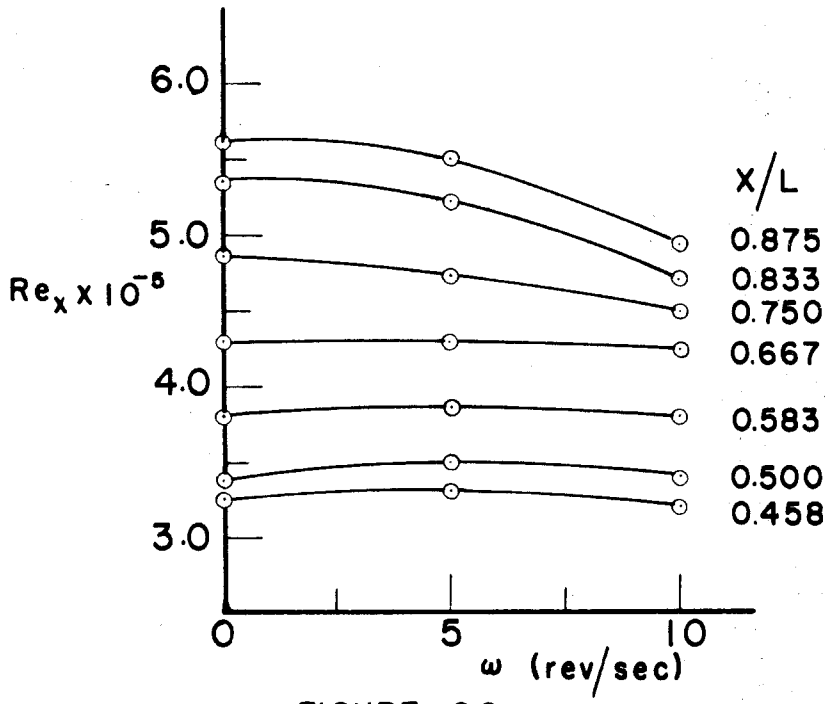

FIGURE 26
Re_x vs. SPIN RATE FOR COMPLETE TRANSITION
$\alpha = 0°$

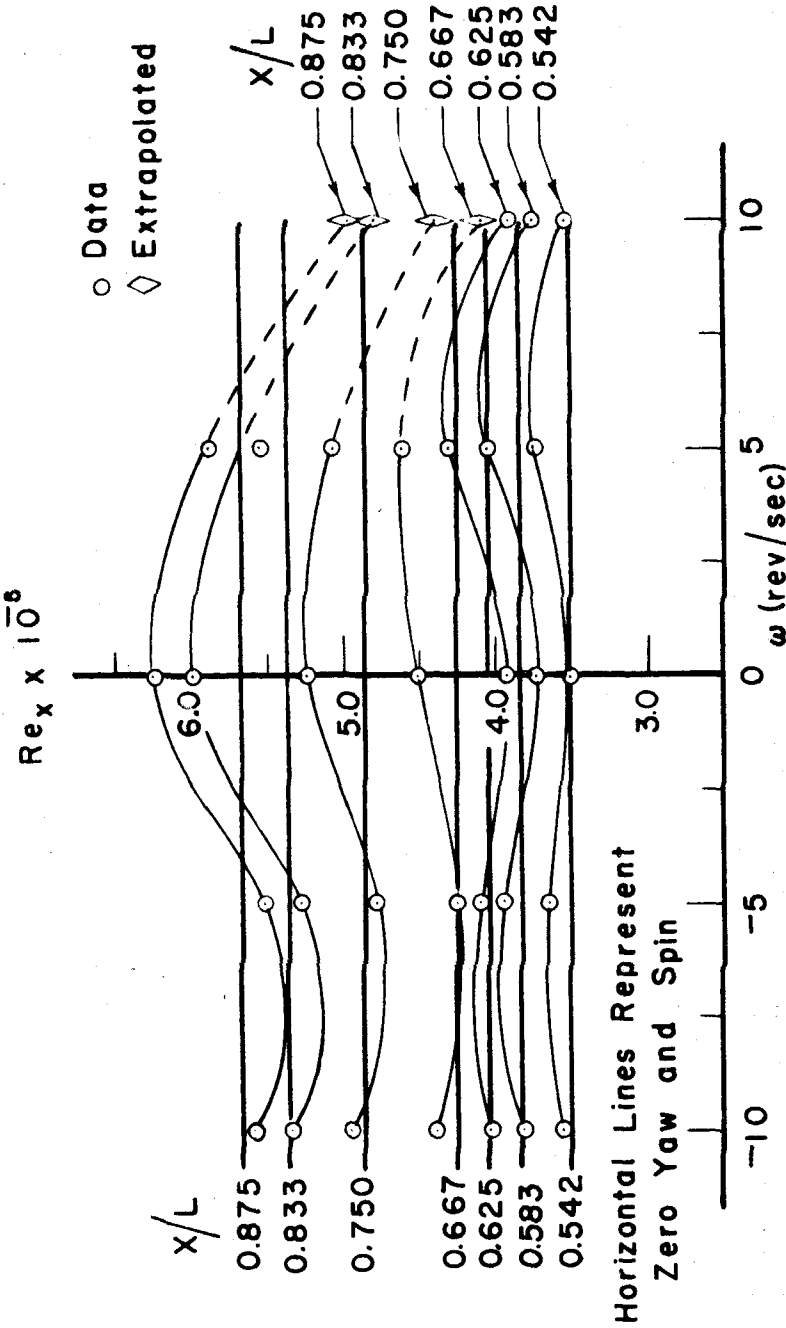

FIGURE 27

Re_x vs. SPIN RATE FOR COMPLETE TRANSITION

$\alpha = 5°$